Research in Astron. Astrophys. **2009** Vol. **9** No. **5**, 585 – 595
http://www.raa-journal.org *http://www.iop.org/journals/raa*

***R**esearch in*
***A**stronomy and*
***A**strophysics*

Turbulence properties in the solar convection envelope: properties of the overshooting regions *

Qian-Sheng Zhang[1,2] and Yan Li[1]

[1] National Astronomical Observatories/Yunnan Observatory, Chinese Academy of Sciences, Kunming 650011, China; *zqs@ynao.ac.cn; ly@ynao.ac.cn*
[2] Graduate School of the Chinese Academy of Sciences, Beijing 100049, China

Received 2008 May 29; accepted 2009 February 23

Abstract We apply the turbulent convection model (TCM) to investigate properties of turbulence in the solar convective envelope, especially in overshooting regions. The results show TCM gives negative turbulent heat flux $\overline{u_r' T'}$ in overshooting regions, which is similar to other nonlocal turbulent convection theories. The turbulent temperature fluctuation $\overline{T'T'}$ shows peaks in overshooting regions. Most important, we find that the downward overshooting region below the base of the solar convection zone is a thin cellular layer filled with roll-shaped convective cells. The overshooting length for the temperature gradient is much shorter than that for element mixing because turbulent heat flux of downward and upward moving convective cells counteract each other in this cellular overshooting region. Comparing the models' sound speed with observations, we find that taking the convective overshooting into account helps to improve the sound speed profile of our nonlocal solar models. Comparing the p-mode oscillation frequencies with observations, we validated that increasing the diffusion parameters and decreasing the dissipation parameters of TCM make the p-mode oscillation frequencies of the solar model be in better agreement with observations.

Key words: convection — turbulence — Sun: helioseismology

1 INTRODUCTION

Turbulent convection models (TCMs), which are based on fully hydrodynamic moment equations (Xiong 1979, 1981; Canuto 1997), are introduced to deal with the problem of inherent non-linearity in the Navier-Stokes equations, which gives rise to higher order correlations in the averaged moment equations and results in an infinite number of differential equations. TCMs are thought to be better than mixing-length theory (MLT) in studying convective motion in stars. They can deal with transport effects, dissipation and anisotropy of turbulence which are not properly considered in MLT. Some parameters are introduced into TCMs to calibrate these effects, but they cannot be given by the theory itself. Many experiments and theoretical efforts (Hossain & Rodi 1982; Canuto 1997a) have been made to evaluate these parameters, but it is not well known whether those parameters obtained in ground-based laboratories can be applied in stellar convection zones. A simple approach of the TCM was tested by Li & Yang (2001, 2007) where model parameters were adjusted to study properties of turbulent convection in the solar convective envelope. Their nonlocal solar models (NLSM) series, which used TCM to deal with

* Supported by the National Natural Science Foundation of China.

convection, are compared with the standard solar model (SSM), which relies on the MLT to deal with convection, by comparing their p-mode oscillation frequencies with the observed ones. It was found that p-mode oscillation frequencies of NLSM with large diffusion parameters and small dissipation parameters were in better agreement with observations than those of the SSM (Yang & Li 2007). However, there are two major shortcomings in their NLSM series. Firstly, the TCM is only applied within the solar convection zone, which is defined by the Schwarzschild criterion. Secondly, the TCM's parameters are restricted by numerical difficulties encountered in their NLSM series of solar models. Based on a new numerical approach, larger diffusion parameters and smaller dissipation parameters are adopted in the present paper and the TCM is used both in the convection zone and in overshooting regions in order to see whether the result can be improved further.

The properties of turbulence in overshooting regions have been studied by Xiong & Deng (Xiong 1985; Xiong & Deng 2001; Deng & Xiong 2008) and others (Canuto 1997b). In the present paper, we can see that the TCM we have adopted also gives negative heat flux $\overline{u_r'T'}$ in overshooting regions. We find peaks for turbulent temperature fluctuation $\overline{T'T'}$ in overshooting regions. Investigating properties of the radial component of turbulent kinetic energy in overshooting regions, we find that the overshooting region below the base of the solar convection zone forms a thin layer filled with cellular convective cells. It is found that the overshooting length for $\overline{u_r'T'}$ is much shorter than that of k or $\overline{T'T'}$ due to the cellular structure there. Comparing our solar models with observations, we find that the convective overshooting makes the resulting sound speed be in better agreement.

In the present paper, we outline basic equations for stellar turbulent convection, the numerical scheme incorporating the TCM into the stellar evolution code in Section 2. The turbulence properties in the solar convective envelope and our solar models are detailed in Section 3. Conclusions of the present paper are summarized in Section 4.

2 BASIC EQUATIONS AND NUMERICAL SCHEME

Equations of stellar structure and evolution are (Huang & Yu 1998)

$$\frac{\partial r}{\partial M_r} = \frac{1}{4\pi r^2 \rho}, \tag{1}$$

$$\frac{\partial P}{\partial M_r} = -\frac{GM_r}{4\pi r^4}, \tag{2}$$

$$\frac{\partial L_r}{\partial M_r} = \varepsilon_N - \varepsilon_\nu - c_P \frac{\partial T}{\partial t} + \frac{\delta}{\rho}\frac{\partial P}{\partial t}, \tag{3}$$

$$\frac{\partial T}{\partial M_r} = -\frac{GM_r T}{4\pi r^2 \rho}\nabla. \tag{4}$$

In the equations above, the temperature gradient ∇ is determined by the method that deals with convection. In general, ∇ can be obtained by the MLT proposed by Böhm-Vitense (1953, 1958). In the present work, the TCM described by Li & Yang (2007) is used to get ∇

$$\nabla = \nabla_R - \frac{\rho c_P H_P}{\lambda T}\overline{u_r'T'}, \tag{5}$$

$$\frac{1}{\rho r^2}\frac{\partial}{\partial r}\left(C_s \rho r^2 \frac{k}{\varepsilon}\overline{u_r'u_r'}\frac{\partial \overline{u_r'u_r'}}{\partial r}\right) = \frac{2}{3}\varepsilon + \frac{2\beta g_r}{T}\overline{u_r'T'} + C_k\frac{\varepsilon}{k}\left(\overline{u_r'u_r'} - \frac{2}{3}k\right), \tag{6}$$

$$\frac{1}{\rho r^2}\frac{\partial}{\partial r}\left(C_s \rho r^2 \frac{k}{\varepsilon}\overline{u_r'u_r'}\frac{\partial k}{\partial r}\right) = \varepsilon + \frac{\beta g_r}{T}\overline{u_r'T'}, \tag{7}$$

$$\frac{2}{\rho r^2}\frac{\partial}{\partial r}\left(C_{t1} \rho r^2 \frac{k}{\varepsilon}\overline{u_r'u_r'}\frac{\partial \overline{u_r'T'}}{\partial r}\right) = \frac{T}{c_P}\frac{\partial \overline{s}}{\partial r}\overline{u_r'u_r'} + C_T\left(\frac{\varepsilon}{k} + \frac{\lambda}{\rho c_P}\frac{\varepsilon^2}{k^3}\right)\overline{u_r'T'} + \frac{\beta g_r}{T}\overline{T'^2}, \tag{8}$$

Table 1 Turbulence Parameters of Solar Models (Yang & Li 2007)

C_t	C_e	C_k	C_{t1}	C_{e1}	C_s
1.0	0.25	1.01	0.1	0.15	0.04

$$\frac{1}{\rho r^2}\frac{\partial}{\partial r}\left(C_{e1}\rho r^2\frac{k}{\varepsilon}\overline{u_r'u_r'}\frac{\partial\overline{T'^2}}{\partial r}\right)=\frac{2T}{c_P}\frac{\partial\overline{s}}{\partial r}\overline{u_r'T'}+2C_e\left(\frac{\varepsilon}{k}+\frac{\lambda}{\overline{\rho}c_P}\frac{\varepsilon^2}{k^3}\right)\overline{T'^2}. \quad (9)$$

The above equations are based on second-order moment equations for turbulent convection, which are closed by some model assumptions. These model assumptions introduce six free parameters: C_t and C_e describing dissipation of turbulence, C_k describing the anisotropy of turbulence, and C_s, C_{t1} and C_{e1} describing the diffusion of turbulence. In this paper, C_t and C_e are referred to as dissipation parameters, and C_s, C_{t1}, and C_{e1} are called diffusion parameters. Other symbols hold the same meanings as in Li & Yang (2007).

A modified stellar evolution code, which was originally written by Paczynski and Kozlowski, and updated by Sienkiewicz, is used to calculate solar evolution models. The OPAL equation of state (Rogers 1994; Rogers, Swenson & Iglesias 1996) is used. The OPAL opacity tables (Rogers & Iglesias 1995; Iglesias & Rogers 1996) are used in the region with $\lg T > 3.95$, and Alexander's opacity tables (Alexander & Ferguson 1994) are used in the region with $\lg T < 3.95$. Nuclear reaction rates from Bahcall (1995) are used. The metal abundance is fixed to be 0.02 in our solar models.

The numerical method that we have used to solve the above equations is an iterative one: solving the TCM's equations with given values of the state of matter to get ∇ by the Newton iteration method, then inputting ∇ into the equations of stellar structure and evolution to solve stellar structure using the evolution code. This iterative procedure continues until the difference in value of ∇ between two consecutive iterations is smaller than 10^{-5}. Boundary positions of TCM's equations are of two types: I. Schwarzschild boundaries, II. the inner boundary is set $3H_p$ below the Schwarzschild boundary and the outer boundary is close to the model surface. It means that we solve the TCM's equations in two cases: only within the convection zone, and in the region including both the convection zone and overshooting regions. The boundary conditions of the TCM are chosen to be small values for turbulent correlation quantities. For every solar model, about 3700 mass zones are included and 213 time-steps are evolved from the ZAMS to the present solar age. The solar luminosity and radius are calibrated to their observed values with an accuracy of 10^{-6} by iteratively adjusting the initial helium abundance Y_0 and the mixing-length to local pressure scale height ratio α.

The linear oscillation code developed by Li (1993) is used to calculate the p-mode oscillation frequencies. The observed p-mode oscillation frequency data are downloaded from the web site of the Global Oscillation Network Group (GONG). These data were published on July 13, 2006.

3 PROPERTIES OF TURBULENCE IN SOLAR OVERSHOOTING REGIONS

A simple version of the TCM has been tested by Li & Yang (Li & Yang 2007; Yang & Li 2007). It is found that p-mode oscillation frequencies of their NLSM series of solar models are in better agreement with observed ones than those of SSM, and it is expected that p-mode oscillation frequencies of such models can be further improved by increasing diffusion parameters and decreasing dissipation parameters of the TCM they have adopted. The six parameters of the TCM which were derived from the best model are listed in Table 1. However, some numerical problems were encountered in their work which prevented them from doing so.

By developing a new method to solve the equations of TCM, some of those numerical problems have been solved, so that we can adopt larger diffusion parameters and smaller dissipation parameters. We can use the TCM not only in the convection zone but also in overshooting regions in the present work. Three solar models with the parameters of the TCM shown in Table 2 have been calculated: the NLSM(1) and NLSM(2a) apply the TCM within the convection zone only, and the NLSM(2b) extends the TCM to overshooting regions $3H_p$ below the Schwarzschild boundary at the inner boundary and

Table 2 Turbulence Parameters and the Convection Zone Information of Solar Models

Model	C_t	C_e	C_k	C_{t1}	C_{e1}	C_s	α	Y_0	$R_{\rm bc}\ (R)$	$T_{\rm bc}\ (10^6{\rm K})$
NLSM(1)	0.25	0.10	2.50	0.11	0.20	0.05	0.05852	0.275088	0.72471	2.11849
NLSM(2a)	0.20	0.10	2.50	0.15	0.25	0.10	0.05162	0.275089	0.72470	2.11852
NLSM(2b)	0.20	0.10	2.50	0.15	0.25	0.10	0.05162	0.275085	0.72470	2.11850
SSM							1.642	0.275058	0.72478	2.11819

close to the model surface. Those models also adopt larger diffusion parameters and smaller dissipation parameters than in Table 1, but fix C_k to be 2.50. That is because ∇, which is the only turbulent quantity used in equations of stellar structure and evolution, is insensitive to C_k (Li & Yang 2007).

NLSM(2b) is our first solar model that applies the TCM both in the convection zone and in the overshooting regions. Properties of the TCM in the convection zone have been discussed in detail by Li and Yang (2007), so that we do not repeat them here. Figures 1–2 show turbulent heat flux $\overline{u_r'T'}$ and temperature fluctuation $\overline{T'^2}$ of NLSM(2b) both in the convection zone and in the overshooting regions. Those of NLSM(1) and NLSM(2a) are similar to NLSM(2b) in the convection zone. The behavior of turbulent properties around Schwarzschild boundaries of the convection zone for NLSM(2b) (the inner boundary at $\lg T = 6.326$ and the outer boundary at $\lg T = 3.782$) are indicated in the figures. It can be seen that turbulent heat flux $\overline{u_r'T'}$ is negative in overshooting regions, and there are two peaks for temperature fluctuation $\overline{T'^2}$ in the inner and outer overshooting regions, respectively. Figure 3 shows temperature gradient ∇ around the Schwarzschild boundary of the convection zone. It is found that $\nabla > \nabla_R$ (in the overshooting region) and $\nabla < \nabla_{\rm ad}$ (in the convection zone) around the Schwarzschild boundary. Those properties of turbulence in the overshooting region will be discussed below.

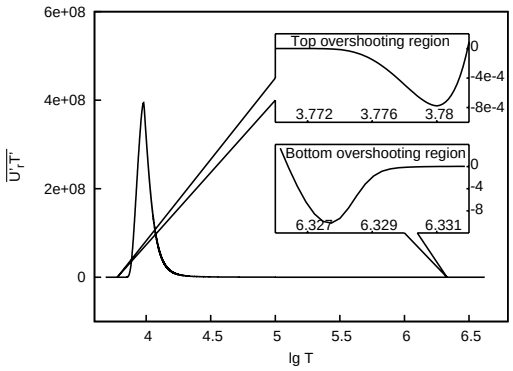

Fig. 1 Turbulent heat flux $\overline{u_r'T'}$ of NLSM(2b).

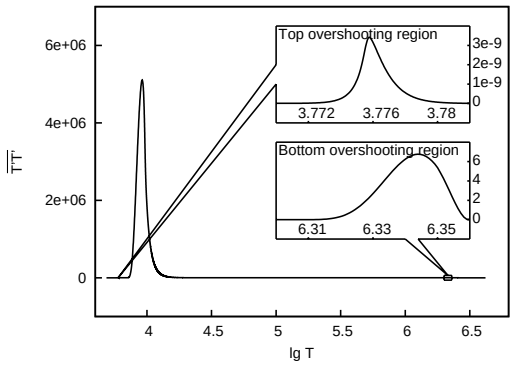

Fig. 2 Turbulent temperature fluctuation $\overline{T'T'}$ of NLSM(2b).

Equations (6)–(9) describe turbulence properties in equilibrium. The left sides of the equations are diffusion terms, and the right side are the generation and dissipation terms. If a term on the right side is positive, it is a dissipative one, otherwise, it is a generative one. We now transform the equations to a more inspiring form for detailed discussions.

When we consider movement of a turbulent fluid element in a star, T_b is its temperature, $U_{r,b}$ is its radial velocity and ρ_b is its density. T_e and ρ_e are the temperature and the density of the environment, and the velocity of the environment is zero $U_{r,e} = 0$. We can find

$$\frac{\delta g_r}{\overline{T}}(T_b - T_e) = -\frac{\rho_b - \rho_e}{\rho_e} g_r = -\frac{d_1 U_{r,b}}{dt}, \tag{10}$$

$$\frac{T}{c_P}\frac{\partial \overline{s}}{\partial r}U_{r,b} = \Big(\frac{\partial \overline{T}}{\partial r} - \frac{\delta}{\overline{\rho} c_P}\frac{\partial \overline{P}}{\partial r}\Big)U_{r,b} = -\frac{\overline{T}}{H_P}(\nabla - \nabla_{\rm ad})\frac{dr}{dt} \tag{11}$$

$$= \frac{\overline{T} d\ln P}{dr_B}\Big(\frac{d\ln T_e}{d\ln P} - \frac{d\ln T_b}{d\ln P}\Big)\frac{dr_B}{dt} \approx -\frac{d_1(T_b - T_e)}{dt}. \tag{12}$$

where, $\frac{d_1}{dt}$ means the time derivative if the dissipation and diffusion of turbulence are not considered.

So, some terms in Equations (6)–(9) can be rewritten as

$$\frac{\delta g_r}{\overline{T}}\overline{T'^2} = \frac{\delta g_r}{\overline{T}}\overline{(T_b - T_e)^2} = -\overline{(T_b - T_e)\frac{d_1 U_{r,b}}{dt}}, \tag{13}$$

$$\frac{\delta g_r}{\overline{T}}\overline{u_r' T'} = \frac{\delta g_r}{\overline{T}}\overline{U_{r,b}(T_b - T_e)} = -\frac{\overline{d_1 {U_{r,b}}^2}}{2dt}, \tag{14}$$

$$\frac{2T}{c_P}\frac{\partial \overline{s}}{\partial r}\overline{u_r' T'} = \frac{2T}{c_P}\frac{\partial \overline{s}}{\partial r}\overline{U_{r,b}(T_b - T_e)} = -\frac{\overline{d_1 (T_b - T_e)^2}}{dt}, \tag{15}$$

$$\frac{T}{c_P}\frac{\partial \overline{s}}{\partial r}\overline{u_r' u_r'} = -\overline{U_{r,b}\frac{d_1(T_b - T_e)}{dt}}. \tag{16}$$

Then Equations (6)–(9) can be rewritten as

$$\frac{1}{\rho r^2}\frac{\partial}{\partial r}\left(C_s \rho r^2 \frac{k}{\varepsilon}\overline{u_r' u_r'}\frac{\partial \overline{u_r' u_r'}}{\partial r}\right) = -\frac{\overline{d_1 {U_{r,b}}^2}}{dt} + \frac{2}{3}\varepsilon + C_k\frac{\varepsilon}{k}\left(\overline{u_r' u_r'} - \frac{2}{3}k\right), \tag{17}$$

$$\frac{1}{\rho r^2}\frac{\partial}{\partial r}\left(C_s \rho r^2 \frac{k}{\varepsilon}\overline{u_r' u_r'}\frac{\partial k}{\partial r}\right) = -\frac{\overline{d_1 {U_{r,b}}^2}}{2dt} + \varepsilon, \tag{18}$$

$$\frac{2}{\rho r^2}\frac{\partial}{\partial r}\left(C_{t1} \rho r^2 \frac{k}{\varepsilon}\overline{u_r' u_r'}\frac{\partial \overline{u_r' T'}}{\partial r}\right) = -\frac{\overline{d_1[U_{r,b}(T_b - T_e)]}}{dt} + C_T\left(\frac{\varepsilon}{k} + \frac{\lambda}{\rho c_P}\frac{\varepsilon^2}{k^3}\right)\overline{u_r' T'}, \tag{19}$$

$$\frac{1}{\rho r^2}\frac{\partial}{\partial r}\left(C_{e1} \rho r^2 \frac{k}{\varepsilon}\overline{u_r' u_r'}\frac{\partial \overline{T^{2\prime}}}{\partial r}\right) = -\frac{\overline{d_1 (T_b - T_e)^2}}{dt} + 2C_e\left(\frac{\varepsilon}{k} + \frac{\lambda}{\overline{\rho} c_P}\frac{\varepsilon^2}{k^3}\right)\overline{T'^2}. \tag{20}$$

In the above equations, terms on the left side are diffusions, ε is the dissipation rate of turbulent kinetic energy, $C_k\frac{\varepsilon}{k}\left(\overline{u_r' u_r'} - \frac{2}{3}k\right)$ the redistribution term containing pressure-strain correlation, $C_T\left(\frac{\varepsilon}{k} + \frac{\lambda}{\rho c_P}\frac{\varepsilon^2}{k^3}\right)\overline{u_r' T'}$ the dissipation rate of $\overline{u_r' T'}$ and $2C_e\left(\frac{\varepsilon}{k} + \frac{\lambda}{\overline{\rho} c_P}\frac{\varepsilon^2}{k^3}\right)\overline{T'^2}$ the dissipation rate of $\overline{T'^2}$ (Li & Yang 2001). $-\frac{\overline{d_1 {U_{r,b}}^2}}{2dt}$, $-\frac{\overline{d_1[U_{r,b}(T_b - T_e)]}}{dt}$ and $-\frac{\overline{d_1 (T_b - T_e)^2}}{dt}$ are the generation rates of kinetic energy, heat flux and temperature fluctuation, respectively.

We can study turbulent properties in the star by analyzing those generation rates. Inside the convection zone, it is obvious that $-\frac{\overline{d_1 {U_{r,b}}^2}}{2dt} < 0$, $-\frac{\overline{d_1 (T_b - T_e)^2}}{dt} < 0$, $-\overline{(T_b - T_e)\frac{d_1 U_{r,b}}{dt}} < 0$, and $-\overline{U_{r,b}\frac{d_1(T_b - T_e)}{dt}} < 0$, so that the four turbulent fluctuations $\overline{u_r' u_r'}$, k, $\overline{u_r' T'}$ and $\overline{T'^2}$ are generated by them. It is easy to see that generation rates are proportional to $\nabla - \nabla_{\rm ad}$, so they are generated significantly in the superadiabatic convection zone. It must be mentioned that the location $\nabla = \nabla_{\rm ad}$ is not the Schwarzschild boundary; there is a region in which $\nabla < \nabla_{\rm ad} < \nabla_R$ near the Schwarzschild boundary shown in Figure 3 (see also Deng & Xiong 2008).

In the overshooting region, we only discuss the downward overshooting region below the bottom of the convection zone. The results are similar for the upward overshooting region above the upper convective boundary, except for those particularly indicated. Buoyancy now prevents movement of an element so that $-\frac{\overline{d_1 {U_{r,b}}^2}}{2dt} > 0$, converting it into a dissipation of turbulent kinetic energy $\overline{u_r' u_r'}$ and k. The temperature of an element moving just across the boundary of the convection zone is approximately

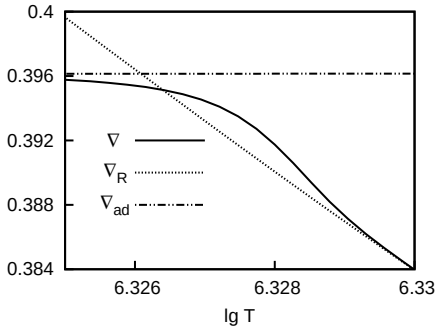

Fig. 3 Temperature gradient of NLSM(2b) around the Schwarzschild boundary of the convection zone.

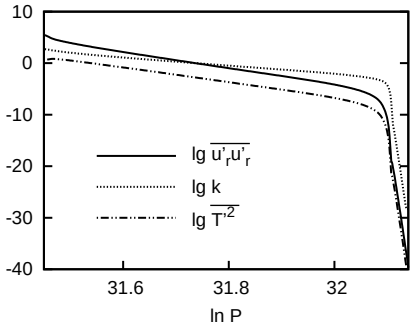

Fig. 4 Downward overshooting length of NLSM(2b).

equal to the environment's ($T_b \approx T_e$), and $\frac{d_1(T_b-T_e)}{dt} > 0$ that results from $\nabla < \nabla_{ad}$ in the overshooting region, and the element is therefore hotter than the environment when it is in the overshooting region, which results in negative heat flux $\overline{u_r' T'}$ shown in Figure 1. However, the position of $\overline{u_r' T'} = 0$ is not identical to the Schwarzschild boundary of the convection zone, because the elements moving at the Schwarzschild boundary of the convection zone are still a little cooler due to turbulent diffusion than those in the environment. Because of the negative heat flux $\overline{u_r' T'}$, we get $\nabla_R < \nabla$ according to Equation (5), and it is obvious that $\nabla < \nabla_{ad}$ in the overshooting region, so that $\nabla_R < \nabla < \nabla_{ad}$ in the overshooting region (Xiong & Deng 2001; Deng & Xiong 2008) which is shown in Figure 3. An element moving in the overshooting region is hotter than the environment ($T_b > T_e$), and $\frac{d_1(T_b-T_e)}{dt} > 0$ which means it gets progressively hotter than the environment in the overshooting region, so $-\frac{\overline{d_1(T_b-T_e)^2}}{dt} < 0$, and $\overline{T'^2}$ increases in the overshooting region, which results in peaks for $\overline{T'^2}$ in overshooting regions as shown in Figure 2. However, because of dissipation of buoyancy, turbulence will finally vanish and all turbulent fluctuations are attenuated to zero.

Overshooting length is an important parameter. The main effects of convective overshooting are mixing of elements and modifying the temperature gradient ∇ by $\overline{u_r' T'}$. For the elements mixing, because the present solar age is about 10^{16} s, and the solar radius is about 10^{10} cm, so that the typical speed for traveling across the sun within the present solar age is about 10^{-6} cm s^{-1}, and it is reasonable to set the location where $\overline{u_r' u_r'} \approx 10^{-12}$ cm^2 s^{-2} to be the boundary of the overshooting region. However, such a definition is reasonable only for the present sun, and it is not a common criterion for all stars. Figure 4 shows the overshooting length of NLSM(2b) below the base of the solar convection zone. The Schwarzschild boundary is at $\ln P \approx 31.45$. We can see $\overline{u_r' u_r'}$, k, and $\overline{T'^2}$ all overshoot to the location where $\ln P \approx 32.1$, $\overline{u_r' u_r'} \approx 10^{-12}$ cm^2 s^{-2} is also at that position, so that the downward overshooting length of NLSM(2b) is about $0.65 H_p$ or $5.2\% R_\odot$, the downward overshooting region of NLSM(2b) is $0.6722 R_\odot < r < 0.7246 R_\odot$. Figure 5 shows the overshooting length of NLSM(2b) above the top of the solar convection zone. The Schwarzschild boundary is at $\ln P \approx 11.63$ or $\lg T \approx 3.782$. We can see $\overline{u_r' u_r'}$, k and $\overline{T'^2}$ all overshoot to the location $\ln P \approx 11.56$ or $\lg T \approx 3.772$, so that the upward overshooting length of NLSM(2b) is about $0.08 H_p$. For $\overline{u_r' T'}$, it can be found in Figure 1 that the overshooting region above the top of the solar convection zone is also $3.772 < \lg T < 3.782$, which is in agreement with the overshooting region of other turbulent quantities. However, the overshooting region of $\overline{u_r' T'}$ is only $6.326 < \lg T < 6.33$ below the base of the solar convection zone, the overshooting length is about $0.02 H_p$ or $0.2\% R_\odot$, which is much shorter than the overshooting length of other turbulent quantities.

Overshooting length is determined by parameters of the adopted TCM. Enlarging the diffusion parameters (C_{t1}, C_{e1}, C_s) or reducing the dissipation parameters (C_t, C_e) is equivalent to increasing generation rates or decreasing dissipation rates of turbulent fluctuations, so that it will amplify the over-

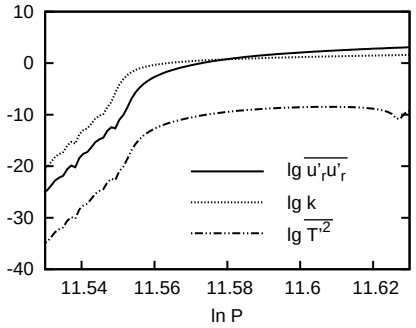

Fig. 5 Upward overshooting length of NLSM(2b).

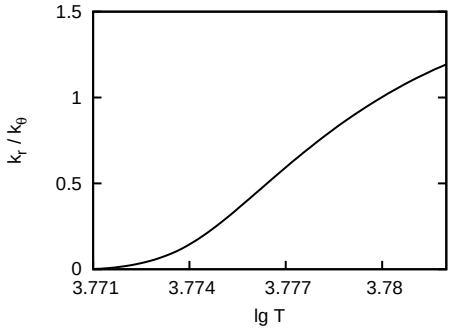

Fig. 6 Ratio of radial kinetic energy k_r to horizontal kinetic energy k_θ in the upward overshooting regions of NLSM (2b).

shooting and increase the overshooting length. Otherwise, reducing the diffusion parameters or enlarging the dissipation parameters will allay the overshooting and decrease the overshooting length. C_s is the most sensitive parameter of TCM in determining overshooting length, because it dominates diffusion of turbulent kinetic energy. In the overshooting region below the base of the convection zone, however, C_{t1} and C_t are insensitive to all turbulent quantities (even $\overline{u_r' T'}$) and their overshooting regions.

The most important result is the discovery of special structure in the overshooting region below the base of the convection zone. Figures 6–7 show the ratio of radial kinetic energy to horizontal kinetic energy in the overshooting regions. It can be found that the ratio of the horizontal component of kinetic energy increasingly dominates in the upward overshooting region, thus fluid elements gradually turn to horizontal movement when they approach the boundary of the upward overshooting region and then return to the convection zone. In the downward overshooting region below the base of the convection zone, however, the horizontal motion dominates only just below the Schwarzschild boundary and near the boundary of the downward overshooting region. This result implies that the downward overshooting region has the structure of a thin cellular layer filled with roll-shaped cells. Changing the TCM's parameters will influence the ratio of radial kinetic energy in the downward overshooting region, but such structure in the overshooting layer is still reserved. That means the downward overshooting region is always a thin cellular layer whatever the TCM's parameters are. Their parameters only determine how many roll-shaped cells are formed in the overshooting region.

In the cellular region, there are both upward and downward flows, but turbulent elements are hotter than the environment in both cases, so upward flow provides positive heat flux to counteract negative heat flux. This effect sharply reduces the effective value of $\overline{u_r' T'}$ in the downward overshooting region, which explains why C_{t1} and C_t are insensitive to the structure of the downward overshooting region and the overshooting length of $\overline{u_r' T'}$ is much shorter than those of other turbulent quantities.

Figure 8 shows the differences in sound speed between models and data of helioseismological inversion techniques. Helioseismological data are obtained by Basu, Pinsonneault & Bahncall (2000). It can be found that the $O - C$ of sound speed of NLSM(2a) is only a little different from that of NLSM(2b). Figure 9 compares sound speed differences of the two models in the solar convective envelope. It can be found that the sound speed difference of NLSM(2b) is smaller than that of NLSM(2a) in the solar convective envelope, especially in the bottom of the solar convection zone and the downward overshooting region. The result indicates that considering convective overshooting improves the sound speed of the models with respect to the observations.

Figures 10–12 show frequency differences of p-mode oscillations with the spherical harmonic index l = 3, 60, 150. It is obvious that the frequency differences of p-mode oscillations of NLSM solar models are reduced more than 30% compared with those of SSM in almost the whole frequency range and for different l. Our results are better than those obtained by Yang & Li (2007) and therefore confirm the

judgment that the p-mode oscillation frequencies of solar models with the TCM can be further improved by increasing diffusion parameters and decreasing dissipation parameters (Yang & Li 2007). It is also found that the $O-C$ of NLSM(2a), which applies the TCM only in the convection zone, is almost identical to that of NLSM(2b), which also applies the TCM in the overshooting regions.

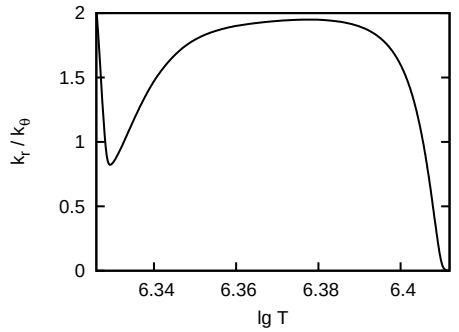

Fig. 7 Ratio of radial kinetic energy k_r to horizontal kinetic energy k_θ in the downward overshooting regions of NLSM(2b).

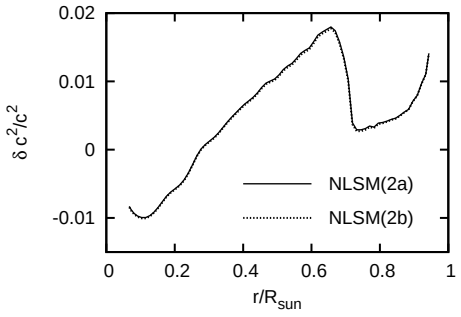

Fig. 8 Differences in sound speed between observation and the two models of NLSM(2a) and NLSM(2b).

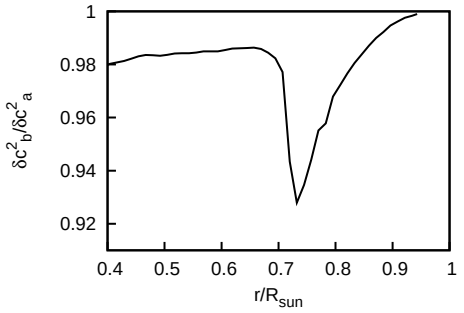

Fig. 9 Comparing the sound speed differences of NLSM(2b) with those of NLSM(2a) in the solar convective envelope.

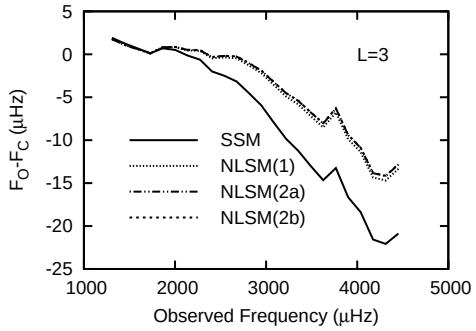

Fig. 10 $O-C$ of p-mode oscillation frequencies of NLSM and SSM at l = 3.

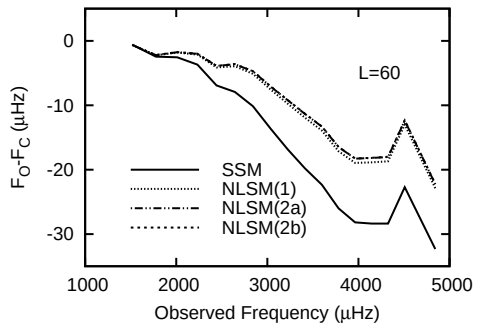

Fig. 11 $O-C$ of p-mode oscillation frequencies of NLSM and SSM at l = 60.

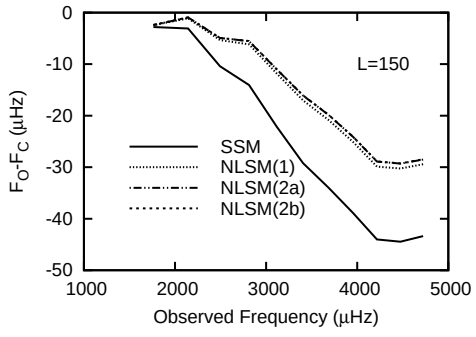

Fig. 12 $O-C$ of p-mode oscillation frequencies of NLSM and SSM at l = 150.

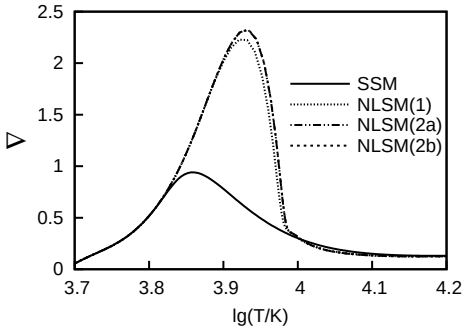

Fig. 13 Temperature gradient of NLSM and SSM in the convection zone.

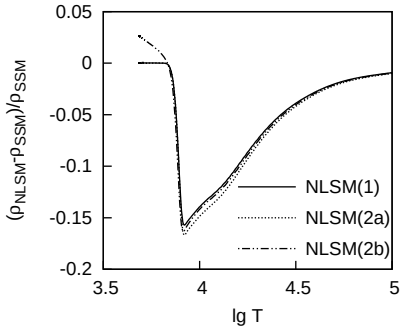

Fig. 14 Differences of density between NLSM and SSM in the convection zone.

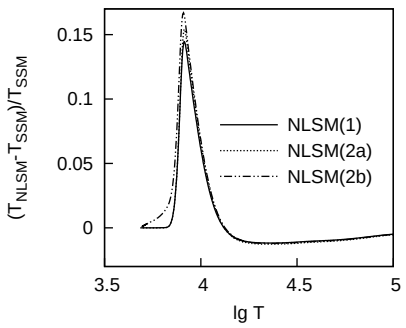

Fig. 15 Differences of temperature between NLSM and SSM in the convection zone.

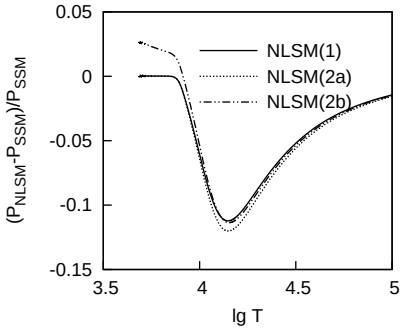

Fig. 16 Differences of pressure between NLSM and SSM in the convection zone.

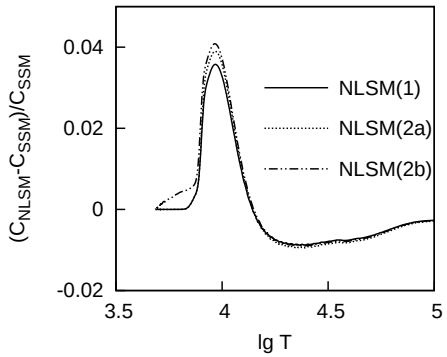

Fig. 17 Differences of sound speed between NLSM and SSM in the convection zone.

Figure 13 shows the temperature gradient in the convection zone. It can be seen that the temperature gradient ∇ increases with an increase of diffusion parameters and a decrease of dissipation parameters in the TCM. The temperature gradient ∇ of NLSM(2a) is also almost identical to that of NLSM(2b).

Figures 14–17 show the relative differences of density, temperature, pressure and speed of sound between NLSM and SSM. Those values of NLSM and SSM are compared at the same r (radius). The

horizontal axes in those figures represent the temperature of SSM in the corresponding r. The relative differences of density, pressure, and temperature reach about 10%–15% near the top of the convection zone, and the relative difference of sound speed in the same region also reaches 3%-4%. Were larger diffusion parameters and smaller dissipation parameters adopted, those differences should increase.

It seems certain that differences in solar p-mode oscillation frequencies between calculated and observed cases can be reduced by increasing diffusion parameters and decreasing dissipation parameters of the TCM. Based on a series of numerical calculations, it has been found that ∇ shows discontinuity when very large diffusion parameters (all set to 1.0) and very small dissipation parameters (all set to 0.1) are adopted. Discontinuous ∇ is considered to be unreal, which implies that the diffusion and dissipation parameters are far away from where they should be. On the other hand, even adopting those parameters, the $O - C$ of p-mode oscillation frequencies shows little improvement compared with NLSM(1), NLSM(2a) and NLSM(2b). Therefore, the best diffusion parameters and dissipation parameters possibly may not be far from NLSM(2a).

4 CONCLUSIONS

Convective overshooting is an interesting and important phenomenon in stars. However, it is usually ignored or excessively simplified in calculations of stellar structure and evolution, because the MLT, which is currently widely used, cannot be applied in the overshooting region because of its neglect of turbulent diffusion. In order to investigate structure of the solar overshooting regions and properties of turbulence in them, we apply the TCM which includes many physical processes ignored in the MLT (Li & Yang 2007) in our solar models in this paper. The main conclusions are summarized as follows.

1. Applying the TCM in the solar overshooting zone shows negative turbulent heat flux $\overline{u_r' T'}$ and results in $\nabla > \nabla_R$ and $\nabla < \nabla_{ad}$ around the Schwarzschild boundary, which is in agreement with Xiong and Deng's results (Xiong & Deng 2001; Deng & Xiong 2008). It is found that $\overline{T'^2}$ shows peaks in the overshooting regions.
2. Investigating the ratio of radial kinetic energy and horizontal kinetic energy in the overshooting regions, we find that the upward overshooting region has a simple structure, and fluid elements gradually turn to horizontal movement in it. However, the downward overshooting region is quite different from the upward one in that it is a thin cellular layer filled with roll-shaped convective cells. In addition, cellular structure always exists regardless of what the TCM's parameters are.
3. Our solar model NLSM(2b) gives a downward overshooting length of $0.02H_p$ for temperature gradient and an overshoot of $0.65H_p$ for the elements mixing. That is similar to Deng and Xiong's (2008) result. The effective overshooting length of $\overline{u_r' T'}$ is much shorter than that of other turbulent quantities in the downward overshooting region, because turbulent heat flux of the upward and downward moving convective cells counteract each other and are almost canceled in the cellular layer below the base of the convection zone. The overshooting length is determined by the TCM parameters, especially the C_s. The downward overshooting length is insensitive to C_{t1} and C_t, because of the counteracting behavior mentioned above.
4. Comparing the models' sound speed with observations, we find that taking the convective overshooting into account helps to improve the profile of sound speed derived from the solar models.
5. In the present work, it is confirmed that frequency differences of solar p-mode oscillation frequencies between the calculated and observed ones can be reduced when increasing diffusion parameters and decreasing dissipation parameters in the TCM of our NLSM models. The $O - C$ of p-mode oscillation frequencies of our two models is reduced more than 30% compared with that of SSM model in almost the whole frequency range and when using a different spherical harmonic degree l.

Acknowledgements Data from solar p-mode frequencies and sound speeds used in this work were obtained by the GONG, National Solar Observatory. Fruitful discussions with J. Y. Yang, H. Y. Xu and J. H. Guo are highly appreciated. This work is co-sponsored by the NSFC through grant 10673030 and the National Key Fundamental Research Project through grant 2007CB815406.

References

Alexander, D. R., & Ferguson, J. W. 1994, ApJ, 437, 879
Bahcall, J. N., Pinsonneault, M. H., & Wasserburg, G. J. 1995, Rev. Mod. Phys., 67, 781
Böhm-Vitense, E. 1953, Z. Astrophys., 32, 135
Böhm-Vitense, E. 1958, Z. Astrophys., 46, 108
Basu, S., Pinsonneault, M. H., & Bahcall, J. N. 2000, ApJ, 529, 1084
Canuto, V. M. 1997a, ApJ, 482, 827
Canuto, V. M. 1997b, ApJ, 489, L71
Deng, L., & Xiong, D. R. 2008, MNRAS, 386, 1979
Hossain, M. S., & Rodi, W. 1982, in Turbulent Buoyant Jets and Plumes, ed. W. Rodi (Oxford: Pergamon Press), 121
Huang, R. Q., & Yu, K. N. 1998, Stellar Astrophysics (New York: Springer)
Iglesias, C. A., & Rogers, F. J. 1996, ApJ, 496, L121
Li, Y., & Yang, J. Y. 2001, ChJAA (Chin. J. Astron. Astrophys.), 1, 66
Li, Y., & Yang, J. Y. 2007, MNRAS, 375, 388
Rogers, F. J. 1994, in IAU Colloquium 147, The Equation of State in Astrophysics, eds. G. Chabrier, & E. Schantzman (Cambridge: Cambridge Univ. Press), 16
Rogers, F. J., Swenson, F. J., & Iglesias, C. A. 1996, ApJ, 456, 902
Rogers, F. J., & Iglesias, C. A. 1995, in ASP Conf. Ser. 78, Astrophysical Applications of Powerful New Databases, eds. S. J. Adelman, & W. L. Wiese (San Francisco: ASP), 78
Xiong, D. R. 1979, Acta Astron Sinica, 20, 238
Xiong, D. R. 1981, Sci. Sinica, 24, 1406
Xiong, D. R. 1985, A&A, 150, 138
Xiong, D. R., & Deng, L. 2001, ApJS, 327, 1137
Yang, J. Y., & Li, Y. 2007, MNRAS, 375, 403